

EPOXY THERMOSETS MODIFIED WITH NOVEL NANO-SCALED, SELF-ASSEMBLED BLOCK COPOLYMERS: TOUGHENING MECHANISMS AND EXTENSION TO COMPOSITES

Nikhil E. Verghese¹, George Jacob¹, Marv Dettloff¹, Ha Q. Pham¹, Jia Liu², Hung-Jue Sue², Zachary J. Thompson³, Frank S. Bates³, John F. Mandell⁴ and Daniel Samborsky⁴

¹*Epoxy R&D, The Dow Chemical Company, Freeport, Texas 77541,*

²*Polymer Technology Center, Department of Mechanical Engineering, Texas A&M University, College Station, Texas 77843*

³*Department of Chemical Engineering and Material Science, University of Minnesota, Minneapolis, MN 55455*

⁴*Montana State University, 301 Cobleigh Hall, Bozeman, MT 59717*

Abstract

A unique approach to toughening thermosets has been identified by introducing small amounts of amphiphilic block copolymer. The result is a good viscosity-Tg-toughness balance. In this paper, the fracture behavior of these modified epoxies, was carefully studied in an attempt to understand the toughening mechanisms that exist. The findings suggest that cavitation in even these nano-sized spherical micelles is the primary mechanism of toughening. These findings were also found to be a strong function of the crosslink density of the host network with higher levels of plastic deformation at the crack tip being observed in the low crosslink density systems. Glass fiber reinforced composites made with epoxies modified with these toughening agents were found to have improved fatigue resistance.

Introduction

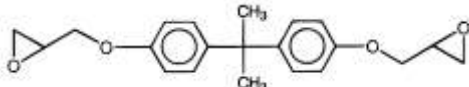
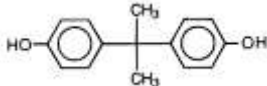
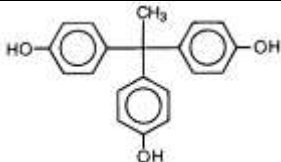
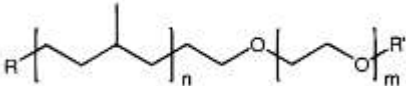
In an attempt to take more complete advantage of epoxy thermosets it is important to improve its toughness. Toughening of such brittle polymers *via* incorporation of a dispersed elastomeric phase is well known as an effective method to improve fracture resistance and impact strength.¹⁻⁴ In rubber-modified plastics, voiding can occur inside the rubber particles under hydrostatic tension. This can be manifested by a macroscopic phenomenon of stress-whitening. Once the rubber particles cavitate, the hydrostatic tension near the cavitation sites is relieved, especially at the crack tip region. The stress state of the matrix near the voids is then transformed from a triaxial stress state to a biaxial stress state, which favors the initiation of shear bands.⁴⁻⁶ Thus, although cavitation in itself cannot be regarded as a significant energy-absorbing process, the real role of cavitation is to relieve the triaxial stress thereby facilitating the matrix shear banding. Since Sultan and McGarry's⁷ early work, many researchers have studied the importance of rubber particle size on toughening for a variety of polymers.^{7, 32-37} Pearson and Yee⁸ found that particles $\geq 20 \mu\text{m}$ in diameter are ineffective for toughening ductile epoxy matrices. On the other hand, for small particle sizes, Bucknall and coworkers⁹⁻¹¹ have proposed a model based on an energy balance concept, showing that the cavitation process in the rubber particles cannot occur with particles less than 250 nm in diameter. Experimentally, the smallest rubber particle size that has been shown to cavitate is 100 nm based on core-shell rubber-modified epoxy systems.¹²⁻¹³ Recently, Bates

and coworkers¹⁴⁻¹⁶ discovered that amphiphilic di-block copolymers (BCP) that self assemble into micellar structures are effective as nano-domain tougheners for epoxy resins. Similar work on triblock copolymer toughened epoxies has also been reported recently.¹⁷⁻¹⁸ However, knowledge of the toughening mechanisms responsible for such toughening effect is still lacking. In addition while rubber particles have been shown to toughen cured epoxies, not all systems can be toughened to the same extent. The concept of *toughenability* has been found to be directly connected to the crosslink density of the cure epoxy network. It is known that the crosslink density of a cured thermoset generally dictates its intrinsic ductility and since matrix shear banding has been identified as the major energy dissipation process in rubber toughened epoxies,^{5, 6, 8, 19} it is not difficult to understand that modifying the matrix ductility can change its toughenability. The present work is part of a larger effort to understand the fundamentals of structure-property relationship in a model epoxy system containing poly(ethylene-*alt*-propylene)-*b*-poly(ethylene oxide) (PEP-PEO) BCP nanoparticles.

Experimentation

Materials: The CET (controlled epoxy thermoset) epoxy chemistry used for the clear casting part of this study consisted of three components: diglycidyl ether of bisphenol-A (DGEBA)-based epoxy monomer (D.E.R.[™] 332 epoxy resin, Dow Chemical), bisphenol-A (BPA) chain extender (PARABIS[™], Dow Chemical), and 1,1,1-tris(4-hydroxyphenyl)ethane crosslinker (THPE, Aldrich). The chemical structures of these reactants are given in Table 1.

Table 1: Chemical structures of epoxy resin, chain extender, crosslinker and block copolymer used in this investigation.

Product	Chemical Structure
DGEBA epoxy resin	
BPA chain extender	
THPE crosslinker	
PEP-PEO block copolymer	 R = <i>s</i> -butyl or <i>t</i> -butyl R' = H or CH ₃

This system was chosen primarily to maintain control over the crosslinked network structure and enable us to vary it in a systematic manner. Realistic formulations make this task very difficult to achieve and results in complicated data interpretation. It is noted that ethyltriphenylphosphonium acetate (70% in methanol, Alfa Aesar) was utilized as a catalyst to promote reactions between primary epoxide groups in the epoxy resin and phenolic functionalities in the chain extender and the crosslinker. This largely reduced the chances of branching reactions with secondary hydroxyl groups, leading to a more uniform and

[™] Trademark of The Dow Chemical Company

controlled epoxy network. As a toughening agent, the PEP-PEO amphiphilic BCP was synthesized using a multi-step polymerization method previously described by Hillmyer and Bates.²⁰ The crosslink density of the cured network was systematically changed by changing the ratio of BPA to THPE and this is reflected in the number designated to the term CET in Table 2.

Preparation of BCP-Modified Epoxy Plaques and Composites: The procedure for sample preparation has been reported in detail earlier¹⁹ so it is only briefly described here. The BCP was mixed and completely dissolved in the epoxy resin at around 150 °C. Then, the chain extender and crosslinker were added into the mixture and dissolved. After degassing, the catalyst was added and the mixture was cured in a pre-heated mold for 2 h at 200 °C.

Glass fiber composites were fabricated using the Vacuum Assisted Resin Transfer Molding (VARTM) process. The epoxy infusion system consisted of a liquid epoxy resin (diglycidyl ether of bisphenol A, DGEBA) and an epoxy-functional reactive diluent that is cured using a mixture of different amine curing agents. The glass fiber used was Knytex[®] DBM1708 (double biased mat) which has a +/-45° fabric with a random mat (RM). The lay up employed was [(RM/-45°/+45°)/(-45°/+45°/RM)]₃ resulting in the laminate having an average thickness of 4.9 mm and a fiber volume fraction of about 40%. The same amphiphilic block copolymer toughening agent employed for the unfilled system study was used for fabricating the toughened composites. The toughening agent was added at 5 wt% of the epoxy resin matrix. The composite panels were cured at 90°C for 24 hours.

Dynamic Mechanical Analysis (DMA): DMA was performed using an RSA III instrument (TA Instruments) at temperatures ranging from -120 to 200 °C with 5 °C per step increase. The tests were performed at a fixed frequency of 1 Hz.

Fracture Toughness Measurement: To obtain the Mode-I critical stress intensity (K_{IC}) of the neat and modified epoxy samples, a single-edge-notch three-point-bending (SEN-3PB) test was performed using the linear elastic fracture mechanics (LEFM) approach in accordance with the ASTM D5045 standard. The dimensions of test specimens are 75 × 12.7 × 3.5 mm³.

Toughening Mechanisms Investigation: The double-notch four-point-bending (DN-4PB) technique was utilized to investigate the detailed toughening mechanisms of BCP-modified epoxy resins with various crosslink densities. Detailed description of this technique can be found elsewhere.¹⁹ The tests were conducted at a crosshead speed of 0.508 mm/min and at room temperature, on an MTS Insight machine. Thin sections with a thickness of ca. 40 μm from the core region of the DN-4PB subcritical crack tip damage zone were obtained by sectioning and polishing, following the procedures described by Holik et al.²¹ Optical microscopy (OM) images were then taken under both bright field and cross-polarized field modes using an Olympus BX60 optical microscope. For transmission electron microscopy (TEM) observation, a block containing a subcritical crack tip damage zone was isolated from the specimen and embedded in an Epo-Fix embedding resin (Electron Microscopy Sciences). Detailed procedure for the preparation and staining of the samples can be found elsewhere.²⁰ TEM micrographs were taken from the stained sections using a JEOL 1200 EX electron microscope operated at an accelerating voltage of 100 kV.

Fatigue Testing of Composites

Fatigue tests were performed using an Instron servo-hydraulic testing machine on rectangular coupon geometries, 25 mm (1 inch) wide and 203 mm (8 inches) long. No additional tab material was applied to the test coupons. The tests were run under sine-wave, load control, constant amplitude using an R value (minimum stress/max stress) of 0.1. The frequency was varied approximately inversely with maximum load to maintain a constant load rate. Frequencies were in the 1 to 3.5 Hz range to avoid significant heating; surface temperatures were monitored for selected tests, and fatigue specimens were surface cooled with fans. The fatigue samples were tested in replicates of 3.

3. Results and Discussion

The results obtained from the fully cured clear castings are captured in Table 2. The numbers after CET indicate the molecular weight between crosslinks in the final cured thermoset - higher the number, lower is the crosslink density.

The fracture toughness is seen to increase with the addition of the BCP toughening agent with minimal loss in Young's modulus at room temperature, which is consistent with the results obtained from DMA. However the magnitude of improvement (toughenability) is a strong function of the crosslink density of the host network.

Figure 1 indicates that the presence of BCP has resulted in pronounced shear yielding of the epoxy matrix, with a lower yield stress. The increase in ductility and drop of yield stress is an early indication that this material will facilitate the formation of crack tip blunting.

Table 2: Storage modulus (E'), T_g and fracture toughness (K_{IC}) of the samples.

Sample	E' (Pa)			T_g (°C)	K_{IC} (MPa·m ^{1/2})
	At low temp.	At room temp.	At rubbery plateau		
CET900	3.27×10^9	1.99×10^9	1.79×10^7	125	0.82 ± 0.05
CET1550	3.86×10^9	2.25×10^9	1.33×10^7	115	0.96 ± 0.04
CET2870	2.80×10^9	2.04×10^9	3.20×10^6	110	0.94 ± 0.03
CET900/BCP	4.07×10^9	2.31×10^9	1.68×10^7	120	1.95 ± 0.03
CET1550/BCP	4.04×10^9	2.36×10^9	9.38×10^6	110	2.73 ± 0.08
CET2870/BCP	3.87×10^9	2.27×10^9	4.38×10^6	100	3.02 ± 0.17

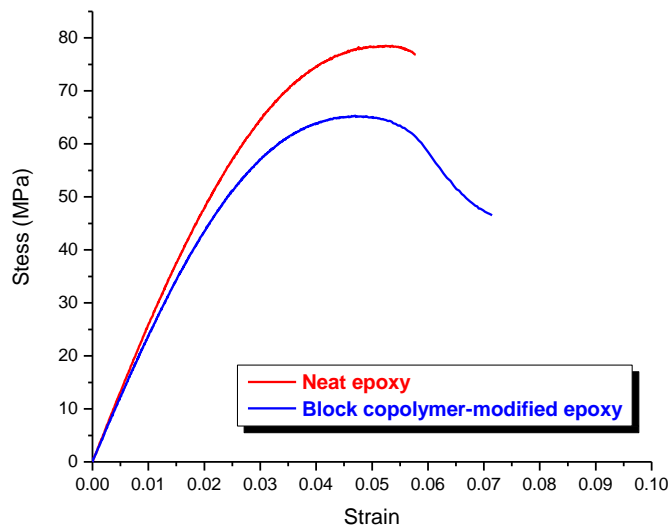


Figure 1: Engineering stress-strain curves of neat epoxy and BCP-toughened epoxy ($M_c=1550$).

Examination of the failure surface of single edge notch bend fracture samples via optical microscopy (Figure 2) shows direct evidence of stress whitening ahead of the initial crack line for the sample modified with BCP. This stress-whitening phenomenon is indicative of the existence of some form of cavitation in the crack tip region and is consistent with the introduction of the strong yielding behavior seen in Figure 1.

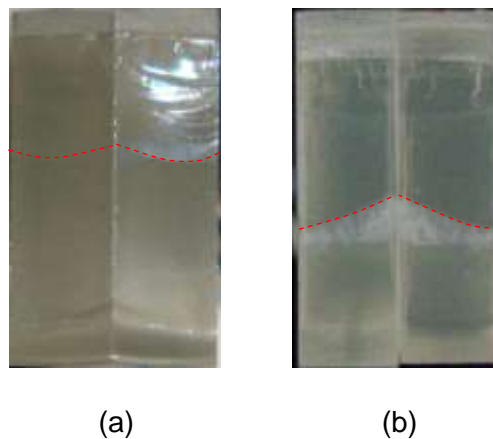
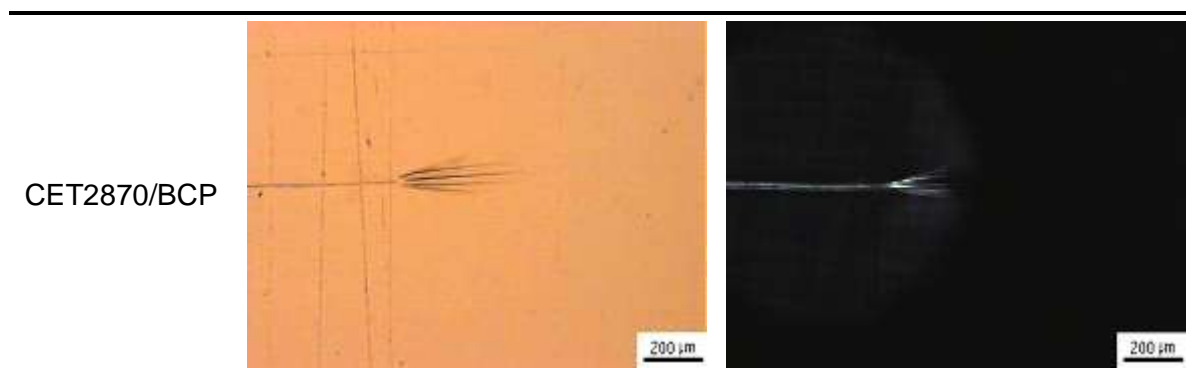
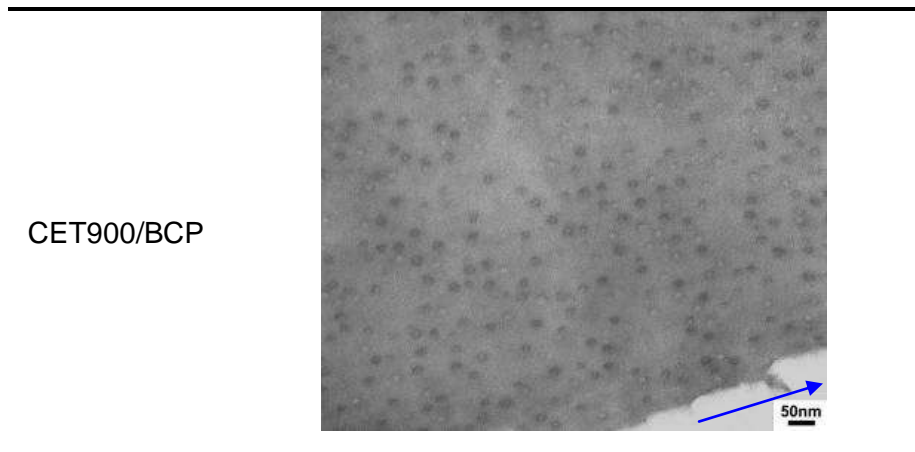
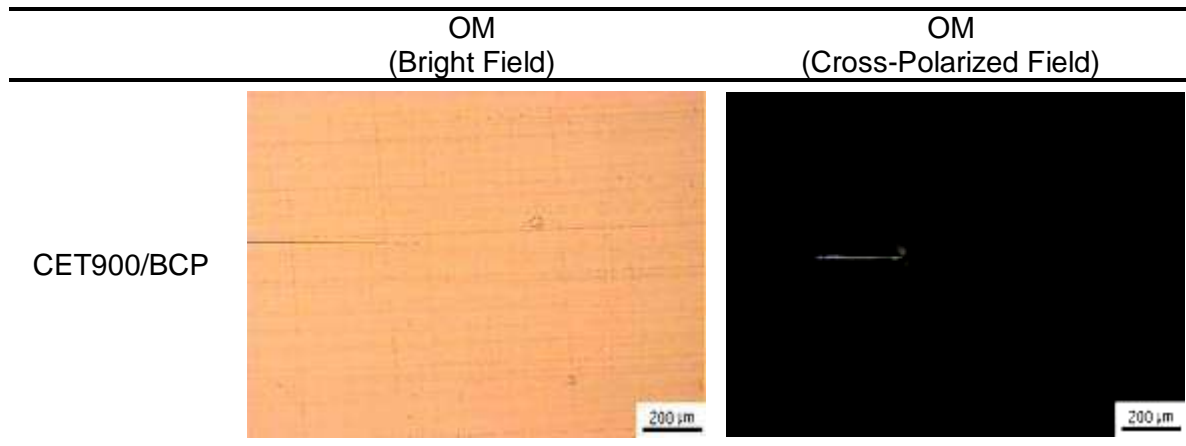


Figure 2: Fracture surfaces of (a) neat epoxy and (b) BCP-toughened epoxy after SEN-3PB tests. A stress-whitening zone was clearly observed in front of the initial crack, as seen in (b). The dashed lines represent the initial crack marks.

Detailed observation suggests that the cavitation takes place inside the BCP phase, not at the micelle-epoxy interface (Figure 3). This cavitation phenomenon is consistent with the stress-whitening feature shown in Figure 2. Since the BCP micelles show significant shape changes, this suggests that the epoxy around the BCP micelles have undergone a significant amount of shear deformation resulting in inelastic deformation. As a result, a cavitation-induced matrix shear banding process is believed to at least partially account for the effective toughening of BCP-toughened epoxy. It is important to mention that the **nano-cavitation** phenomenon observed in the 15 nm BCP particles is the smallest rubber particle size experimentally shown to cavitate and to promote shear banding of a polymer matrix. All

the information obtained from OM and TEM observations is consistent with the fracture toughness results. It is also evident that the particle cavitation and matrix shear banding mechanisms are highly suppressed for the high crosslink density (low M_c) epoxies. The higher the M_c the more flexible the network architecture becomes. This means it is more likely that the material can undergo plastic deformation and dissipate more fracture energy through intermolecular motions.



CET2870/BCP

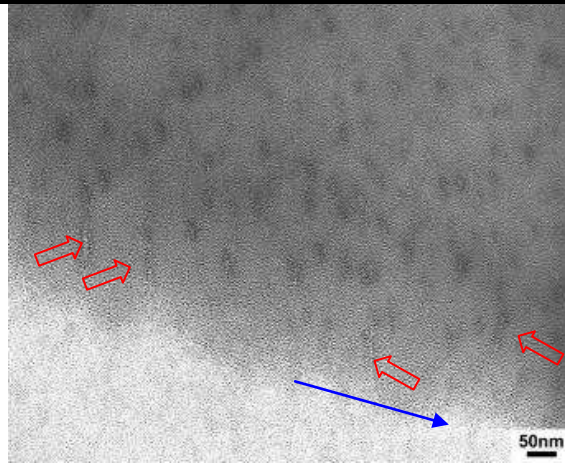


Figure 3: OM images of subcritical crack tip regions as well as TEM micrographs taken in the vicinity of subcritical crack tips in CET900/BCP and CET2870/BCP, respectively. The specimen thin-sections were stained using 0.5% RuO₄ aqueous solution prior to TEM imaging. The crack propagating directions are indicated in the images. In the CET2870/BCP image, the arrows point to the BCP nanoparticles that are severely stretched.

In order to determine how toughness improvements made at the unfilled plaque level translate to the composite level, tension-tension fatigue response curves were generated on glass fiber composites using both the toughened and untoughened systems. The test protocol is described in a previous section of this paper. The matrix while still being epoxy based is not identical to the one used to generate the clear casting information described previously in this paper. The hardener was changed from a phenolic (solid) to an amine (liquid) to facilitate VARTM fabrication of composite panels. Figure 4 presents the data in terms of normalized maximum tensile stress (applied stress/tensile strength) vs. log cycles to failure. Failure during the fatigue tests was determined as complete separation of the test coupon. The results are then represented with the help of a power law fit of the form, $S = AN^B$ where S is the normalized stress (applied stress as a percentage of the tensile strength of the composite), N is cycles to failure, and A and B are constants. It can clearly be seen that the number of cycles to failure, i.e. life of the composite for the toughened composite was more than twice the untoughened version at lower stress levels. While research in this area is still “work in progress”, initial results are revealing that considerable improvements in composite fatigue resistance can be made when using block copolymer toughening for composite applications.

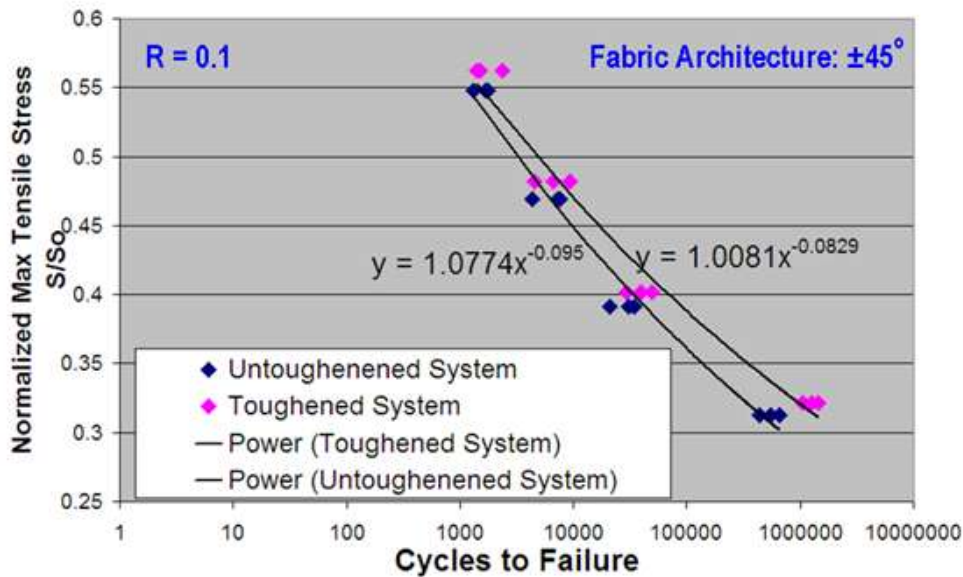


Figure 8:

Tensile fatigue results for the toughened and untoughened composite panels.

Summary and Conclusions

A PEP-PEO diblock copolymer at 5 wt% loading was utilized to toughen bisphenol-A type of epoxy. The BCP self-assembled into ca. 15 nm spherical micelles that were well dispersed in the matrix. Mechanical characterization indicates that the PEP-PEO diblock copolymer can greatly improve the fracture toughness of epoxy without compromising its modulus. The DN-4PB test and TEM observation suggest that the major toughening mechanisms in BCP-toughened epoxy include copolymer micelle cavitation followed by matrix shear banding. The fundamental cause(s) for such a small-scale cavitation process is yet to be determined. The likely contributing factors for the observed nano-scale cavitation phenomenon may include the unique BCP micelle structural characteristics and a possible influence of the surrounding epoxy network, which is significantly modified by the PEO block. The findings also suggest that the toughenability of the epoxy resin has a strong dependence on its M_c . The lower the crosslink density is, the more capable the host resin can be toughened by the incorporation of the elastomeric phase. It is possible to develop a high performance thermosetting material with combined desirable T_g , modulus and toughenability. Additional work is still needed to understand the physical nature of network formation and its interactions with BCP particles at nanometer scale, especially at their interphase.

While work is currently ongoing, it is clear that fracture toughness improvements registered at the clear casting level does translate to the composite level in the form of enhanced mechanical fatigue resistance. Therefore, this toughening approach can have a very positive impact on cycle time reduction (reduction in formulation viscosity) and toughness of epoxy based composites in structurally demanding applications in automotive and adjacent transportation especially those that experience repeated mechanical loading over its service life.

References

- [1] Bucknall, C. B., *Toughened Plastics*. Applied Science: London, 1977.
- [2] Bascom, W. D.; Cottington, R. L.; Jones, R. L.; Peyser, P. *J. Appl. Polym. Sci.* **1975**, 19, 2545.
- [3] Kinloch, A. J., In *Toughened Plastics*, Riew, C. K., Ed. Adv. in Chem. Ser.: 1989; Vol. 67, p 222.
- [4] Sue, H. J.; Yee, A. F. *Polym. Eng. Sci.* **1996**, 36, 2320.
- [5] Yee, A. F.; Pearson, R. A. *J. Mater. Sci.* **1986**, 21, 2462.
- [6] Pearson, R. A.; Yee, A. F. *J. Mater. Sci.* **1986**, 21, 2475.
- [7] Sultan, J. N.; McGarry, F. J. *J. Polym. Eng. Sci.* **1973**, 13, 29.
- [8] Pearson, R. A.; Yee, A. F. *J. Mater. Sci.* **1991**, 26, 3828.
- [9] Lazzeri, A.; Bucknall, C. B. *J. Mater. Sci.* **1993**, 28, 6799.
- [10] Bucknall, C. B.; Karpodinis, A.; Zhang, X. C. *J. Mater. Sci.* **1994**, 29, 3377.
- [11] Lazzeri, A.; Bucknall, C. B. *Polymer* **1995**, 26, 2895.
- [12] Sue, H. J.; Puckett, P. M.; Bertram, J. L.; Walker, L. L.; Garcia-Meitin, E. I. *J. Polym. Sci., Part B: Polym. Phys.* **1999**, 37, 2137.
- [13] Gam, K. T.; Miyamoto, M.; Nishimura, R.; Sue, H. J. *Polym. Eng. Sci.* **2003**, 43, 1635.
- [14] Dean, J. M.; Grubbs, R. B.; Saad, W.; Cook, R. F.; Bates, F. S. *J. Polym. Sci., Part B: Polym. Phys.* **2003**, 41, 2444.
- [15] Dean, J. M.; Verghese, N. E.; Pham, H. Q.; Bates, F. S. *Macromolecules* **2003**, 36, 9267.
- [16] Wu, J.; Thio, Y. S.; Bates, F. S. *J. Polym. Sci., Part B: Polym. Phys.* **2005**, 43, 1950.
- [17] Girard-Reydet, E.; Pascault, J. P.; Bonnet, A.; Court, F.; Leibler, L. *Macromol. Symp.* **2003**, 198, 309.
- [18] Hydro, R. M.; Pearson, R. A. *J. Polym. Sci., Part B: Polym. Phys.* **2007**, 45, 1470.
- [19] Liu, J.; Sue, H.-J.; Thompson, Z. J.; Bates, F. S.; Dettloff, M.; Jacob, G.; Verghese, N.; Pham, H. *Macromolecules* **2008**, 41, 7616.
- [20] Hillmyer, M. A.; Bates, F. S. *Macromolecules* **1996**, 29, 6994.
- [21] Holik, A. S.; Kambour, R. P.; Hobbs, S. Y.; Fink, D. G. *Microstruct. Sci.* **1979**, 7, 357.